



HAL
open science

Optimal production of microalgae in the presence of grazers

Carlos Martínez, Bruno Assis Pessi, Olivier Bernard

► **To cite this version:**

Carlos Martínez, Bruno Assis Pessi, Olivier Bernard. Optimal production of microalgae in the presence of grazers. *Journal of Process Control*, 2022, 118, pp.153-164. 10.1016/j.jprocont.2022.09.001 . hal-03920759

HAL Id: hal-03920759

<https://hal.science/hal-03920759>

Submitted on 3 Jan 2023

HAL is a multi-disciplinary open access archive for the deposit and dissemination of scientific research documents, whether they are published or not. The documents may come from teaching and research institutions in France or abroad, or from public or private research centers.

L'archive ouverte pluridisciplinaire **HAL**, est destinée au dépôt et à la diffusion de documents scientifiques de niveau recherche, publiés ou non, émanant des établissements d'enseignement et de recherche français ou étrangers, des laboratoires publics ou privés.

Optimal production of microalgae in the presence of grazers

Carlos Martínez^{a,*}, Bruno Assis Pessi^b, Olivier Bernard^{b,c}

^a*Institute of Hydrobiology, Biology Centre of the Czech Academy of Sciences, Na Sádkách 7, České Budějovice, Czech Republic*

^b*Université Côte d'Azur, Inria, INRAE, CNRS, Sorbonne Université, Biocore Team, Sophia Antipolis, France*

^c*LOV-UPMC Sorbonne-CNRS, UMR 7093, Station Zoologique, B.P. 28, Villefranche-sur-mer, 06234, France*

Abstract

Zooplankton contamination represents a major constraint in large-scale microalgal cultivation systems. While zooplankton contamination cannot be avoided, their development can be controlled by regulating the dilution rate. However, it is not straightforward to find the best control strategy for the dilution rate. Low dilution rates (or long retention times) favor grazer development and high dilution rates avoid their establishment at the risk of reducing microalgal productivity. Furthermore, the presence of periodic regimes arising from the interaction predator-prey makes it unclear if the presence of grazers must be completely avoided. In this paper, we study the role of the dilution rate in the control of zooplankton populations and in the optimization of biomass productivity. We show that in the long-term operation (static optimal control problem or SOCP), the optimal constant dilution rate must ensure the eradication of the zooplankton population. In the case of time-varying dilution rate, we numerically solve an optimal control problem (OCP) over a finite interval of time. We find that the optimal solution approaches the solution for the SOCP most of the time, except when zooplankton actively avoid the pond outflow. Based on these results,

*Corresponding author

Email addresses: `carlos.martinez@hbu.cas.cz` (Carlos Martínez), `bruno.assis-pessi@inria.fr` (Bruno Assis Pessi), `olivier.bernard@inria.fr` (Olivier Bernard)

we propose a simple sub-optimal feedback control that approximately matches the solution of the OCP when the initial concentration of grazers is low.

Keywords: Biotechnology, Chemostat, Predator-prey, Optimal Control, Biomass productivity, Dilution rate

1. Introduction

Microalgae are a growing natural resource with several commercial applications in the fields of pharmaceuticals, cosmetics up to feedstocks for aquaculture [1]. A challenge when cultivating these organisms, especially in open
5 reactors like raceways, is to limit contamination by other organisms such as viruses, bacteria, fungus, other microalgal species, and grazers [2, 3]. In industrial conditions, it is indeed impossible to operate the process under axenic conditions, and the surrounding environment will permanently bring invaders to the medium. In particular, predators (ciliates, rotifers, daphnia, copepods,
10 etc.) are a poignant issue since they may rapidly develop and lead to a culture crash within a few days [3].

To date, there is no efficient strategy to limit crop loss through zooplanktonic predation, and most of the microalgae grown outdoors in open reactors are extremophiles, which develop in a medium hostile to most of the organisms
15 present in the surrounding ecosystems. Chemical pesticides can limit contamination but they have both high economical and environmental costs. Physical methods are effective, but they are not cost-effective and they can also affect negatively microalgae [4]. An alternative that has scarcely been explored, is the control of the dilution rate. Since species with a generation rate slower than the
20 dilution rate are unlikely to establish in cultivation systems, high dilution rates reduce grazers abundance [5, 6].

The dilution rate (the inverse of the hydraulic retention time) is one of the most important operational variables for continuous cultivation systems [7]. Different authors have studied how to control the dilution rate to maximize
25 biomass productivity. In the absence of predators, when algal growth is limited

only by light, there exists the well-known compensation principle [8, 9]: the productivity is maximal when at the bottom of the culture, the specific growth rate equals the respiration rate. The existence of an optimal dilution rate has been experimentally shown by many authors in the absence of predators [10, 11].
30 Other theoretical works have considered the dilution rate varying in time [12, 13]. Regarding contaminated systems, there are only a few works concerning the impact of the dilution rate [14, 15].

Any control of the dilution rate should consider two important aspects. The first one is that zooplankton often escape the outflow of the pond. For example, cladocerans migrate to near the pond surface at night, resulting in lower
35 densities in the deep water column where the outflow is often located [6, 16]. This has also been observed in chemostat experiments, where cladocerans concentrate near the bottom of the chemostat, remaining below the surface from which the overflow occurs [17]. The critical dilution rate to eradicate some
40 zooplankton populations is therefore higher than their generation rate. Previous theoretical studies assume that microalgae and zooplankton are equally affected by the dilution rate [14, 15, 18], and therefore they may underestimate the impact of grazers. The second important aspect is shared by any predator prey model, that is, the existence of limit cycles. Low dilution rates favor the
45 existence of limit cycles [15]. This is because of the enrichment paradox: favorable conditions for the prey may cause the population to destabilize into a limit cycle [19, 20, 18]. Comparing the productivity along limit cycles with that of equilibria is not trivial. In [15], we numerically show that in the long-term, productivity is higher in the absence of grazers. Therefore, limit cycles cannot
50 be an optimal regime. However, we did not consider that zooplankton may avoid outflow. As shown in this paper, the avoidance of the outflow favors the existence of limit cycles.

In this work, we investigate how to control the dilution rate to maximize the microalgae production in a culture susceptible to predation. We study two
55 cases: (I) the dilution rate is constant and the system is operated in the long-term; (II) the dilution rate is time-varying, and biomass is harvested over a

finite interval of time. In both cases, we consider a chemostat model in which microalgae and grazers grow together (predator-prey model), and we assume that only a fraction of predators is diluted. For Case (I), we determine the
60 necessary and sufficient conditions for the coexistence of both populations, and we show that any solution of the model approaches either an equilibrium or a limit cycle. This allows us to state the static optimal control problem: to find the value of the dilution rate that maximizes the biomass productivity in the long-term (*i.e.* when an attracting set is reached). Using the toolbox Matcont
65 for MATLAB [21], we numerically find the best dilution rate. This is not trivial due to the existence of limit cycles. As we show in this paper, for a fixed dilution rate, limit cycles provide higher biomass productivity than equilibria. For case (II), we use the software BOCOP [22] to numerically solve the optimal control problem of finding the best strategy to maximize the biomass productivity over
70 a finite time interval.

This paper is organized as follows. In Section 2, we describe the microalgae-grazers model. In Section 3, we determine the necessary and sufficient conditions for the survival of predators. In Section 4, we study the steady-state optimization problem of maximizing biomass productivity. In Section 5, we study the
75 optimal control problem of maximizing biomass productivity in a fixed interval of time. In Section 6, we discuss our results. Finally, the conclusion is presented in Section 7.

2. Model description

2.1. Mass balance equations

80 We consider the growth of microalgae (with density x) in a chemostat contaminated by predators of population density y (see Figure 1). The dynamics of both populations is given by the following system of ordinary differential equations

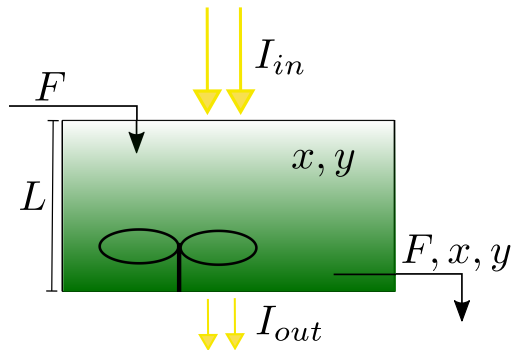


Figure 1: Scheme of a continuous microalgae (x) culture contaminated by predators (y). The culture is illuminated from above with an incident light intensity I_{in} . The culture has a depth L . The light intensity at the bottom is I_{out} . The inlet flow F is equal to the output flow.

$$\frac{dx}{dt} = [\mu(x) - D]x - \frac{1}{\gamma}\nu(x)y, \quad (1)$$

$$\frac{dy}{dt} = [\nu(x) - m - \alpha D]y.$$

The terms μ and ν are the specific growth rate of microalgae and predators, respectively. The parameter $\gamma \in [0, 1]$ corresponds to the assimilation efficiency and m is the mortality rate of predators. The term D is the dilution rate that is defined as the inlet flow (F) divided by the reactor volume (see Figure 1). Finally, the term α is a parameter reflecting the fact that some predators can escape from dilution, for example, by accumulating at a place below the output of the chemostat [17]. This parameter takes values between 0 and 1. If $\alpha = 1$, then algae and predators are equally diluted; however, if $\alpha = 0$, then predators are unaffected by dilution. Along this work, we assume that α is constant in time. While this assumption is reasonable for indoor cultures, where parameters such as light and temperature are kept constant, the main motivation for this assumption is to keep the model simple. Predator-prey models with time-varying parameters may exhibit a chaotic behavior [23].

Table 1: Parameters

Parameter	Value	Unit	Reference
p_{max}	1.68	d ⁻¹	[24]
K_I	108	$\mu \text{ mol m}^{-2} \text{ s}^{-1}$	[24]
r	0.1	d ⁻¹	
k	0.2	$\text{m}^2 \text{ g}^{-1}$	[18]
ν_{max}	1.4	d ⁻¹	[18]
K_x	219	g m^{-3}	[18]
m	0.15	d ⁻¹	[18]
γ	0.21		[18]
L	0.15	m	
I_{in}	1000	$\mu \text{ mol m}^{-2} \text{ s}^{-1}$	
D_{max}	2	d ⁻¹	

2.2. Specific growth rates

The specific growth rate of predators depends on the microalgae concentration as follows:

$$\nu(x) = \nu_{max} \frac{x}{K_x + x}, \quad (2)$$

with ν_{max} the maximal growth rate and K_x a half saturation constant.

The growth rate of microalgae follows from the combination of a light response model and a light distribution model. Light intensity decreases as it passes through the microalgae culture due to absorption and scattering by algal cells [25]. Let L be the depth of the culture, which is illuminated from above as illustrated in Figure 1. In line with standard hypotheses for photolimited photobioreactors [26], light is assumed to be attenuated exponentially according to the Lambert-Beer law. Thus, at a distance $z \in [0, L]$ from the illuminated surface, the corresponding light intensity $I(x, z)$ is given by:

$$I(x, z) = I_{in} e^{-kxz},$$

with $k > 0$ the specific light attenuation coefficient of microalgae. Following [24], the growth rate of microalgae is obtained integrating the local specific growth

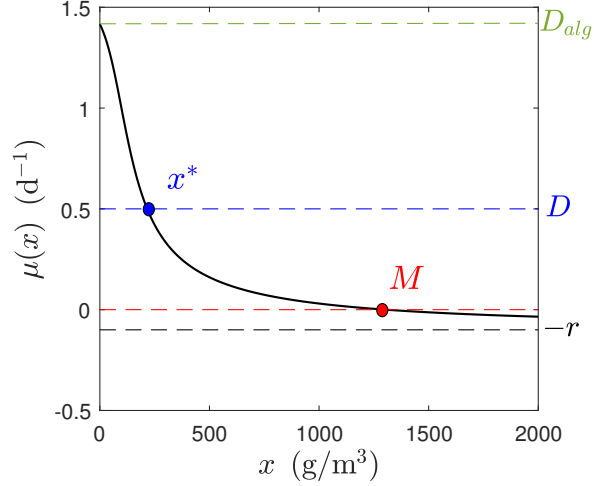


Figure 2: Graphical description of M and x^* defined by (8) and (11), respectively.

rates over all the culture

$$\mu(x) := \frac{1}{L} \int_0^L p(I(z, x)) dz - r, \quad (3)$$

where $p(I)$ corresponds to the light response of microalgae and $r > 0$ is the respiration rate. The function $p(I)$ is described by a Monod model:

$$p(I) = p_{max} \frac{I}{K_I + I}, \quad (4)$$

where $K_I > 0$ is a half-saturation constant, and $p_{max} > 0$ is the maximal specific growth rate. Parameters of the model are given in Table 1.

The following lemma establishes some basic properties of the specific growth rate of microalgae.

Lemma 1. *The function $\mu : [0, \infty) \rightarrow \mathbb{R}$ defined by (3) is continuous, strictly decreasing, and $\lim_{x \rightarrow \infty} \mu(x) = -r$.*

Proof. See Appendix C in [27]. □

From Lemma 1, we have that μ is strictly decreasing (see also Figure 2). This property reflects the self shading effect, that is, as microalgae concentration increases, the light availability in the medium decreases, thus reducing the

growth rate. This implies that $\mu(0)$ is the maximal hypothetical growth rate of microalgae at which they tend to grow as their concentration decreases and the medium becomes transparent. From (3), we have that

$$\mu(0) = p(I_{in}) - r. \quad (5)$$

The light intensity I_{in} is assumed to be large enough such that microalgae can grow (gross growth rate larger than respiration), and therefore we assume that

$$\mu(0) > 0. \quad (6)$$

When $x > 0$, we can integrate (3) to obtain

$$\mu(x) = \frac{\mu_{max}}{kxL} \ln \left(\frac{K_I + I_{in}}{K_I + I_{out}(x)} \right) - r, \quad x > 0. \quad (7)$$

with $I_{out}(x) = I(x, L)$ the light intensity at the bottom of the culture.

Using Lemma 1 and (6), we have the existence of a unique $M > 0$ such that (see Figure 2):

$$\mu(M) = 0. \quad (8)$$

If the microalgae concentration is higher than M , then respiration (r) exceeds the average photosynthesis along the column, and the specific growth rate μ becomes negative. Thus, the quantity M represents the maximum population density that can be reached by microalgae at steady state (replace D and y by zero in (1)). In this paper, we are interested in the case where predators can develop in the reactor, therefore we assume

$$\nu(M) > m. \quad (9)$$

If (9) does not hold, predators will naturally disappear from the reactor in the long-term.

3. Establishment of predators

110 3.1. Dynamics in the absence of grazers

To determine conditions for the establishment of predators in the chemostat, we begin describing the situation in which microalgae grow in the absence of

predators, that is, we replace y by zero in (1). The dynamics of microalgae is then given by the following one-dimensional differential equation:

$$\frac{dx}{dt} = [\mu(x) - D]x. \quad (10)$$

If $\mu(0) > D$, since μ is strictly decreasing (Lemma 1) and $\mu(M) = 0$, there is a unique $x^* > 0$ such that (see Figure 2):

$$\mu(x^*) = D. \quad (11)$$

It is clear that x^* is globally asymptotically stable (GAS) with respect to (10) on $(0, \infty)$. Sometimes we will write $x^*(D)$ instead of x^* to emphasize the fact that x^* depends on the dilution rate. On the other hand, if $\mu(0) \leq D$, then any solution to (10) converges to 0. Thus, the dilution rate $D_{alg} := \mu(0)$ represents the minimal dilution rate at which microalgae are washed out from the culture (see Figure 2). The equilibrium (of (1)) characterized by the presence of microalgae and the absence of predators, whenever it exists, will be denoted by

$$E^* = (x^*, 0). \quad (12)$$

3.2. Coexistence of microalgae and predators

The following proposition answers the question whether microalgae and predators coexist in the long-term.

Proposition 1 (Coexistence). There is a dilution rate $D_{coex} \in (0, D_{alg})$ such
 115 that

- (a) If $0 < D < D_{coex}$, then there is a unique coexistence equilibrium $E_c = (x_c, y_c)$, and any solution to (1) approaches asymptotically either E_c or a positive periodic solution.
- (b) If $D_{coex} \leq D < D_{alg}$, then there is no coexistence equilibrium, and any
 120 solution to (1) approaches E^* asymptotically.
- (c) If $D_{alg} < D$, then any solution approaches asymptotically $(0, 0)$.

PROOF. See Appendix A. \square

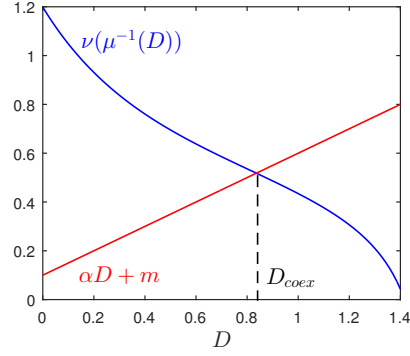


Figure 3: Graphical representation of D_{coex} . As α or m decreases, the value of D_{coex} increases.

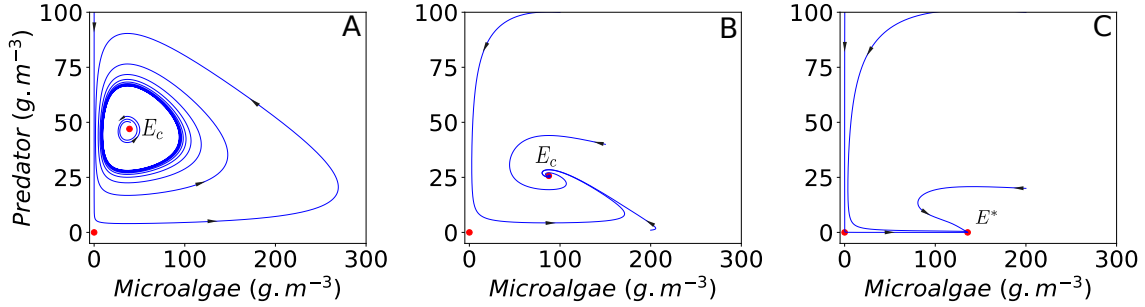


Figure 4: Possible asymptotic behaviors of the solutions of (1) when $\alpha = 0.5$. **A.** The coexistence equilibrium E_c exists and is unstable ($D = 0.1 d^{-1}$), and solutions approach a limit cycle. **B.** The coexistence equilibrium E_c exists and is stable ($D = 0.5 d^{-1}$). **C.** There is no coexistence equilibrium ($D = 0.8 d^{-1}$)

Proposition 1 shows the existence of a dilution rate D_{coex} that characterizes the long-term coexistence of microalgae and zooplankton. Note that since
125 zooplankton needs microalgae to grow, the survival of predators is equivalent to the coexistence of both populations.

The value of D_{coex} can be determined from the following system of equations for x^* and D (see the proof of Proposition 1):

$$\begin{aligned}\mu(x^*) &= D, \\ \nu(x^*) &= m + \alpha D.\end{aligned}\tag{13}$$

From Lemma 1, we have that the inverse of μ exists. Thus, from the first equation in (13), we can write $x^* = \mu^{-1}(D)$. Then, D_{coex} is obtained as the intersection between the line $m + \alpha D$ and the function $D \mapsto \nu(\mu^{-1}(D))$ (see
130 Figure 3). We note that low values of α (longer retention time of grazers in the reactor) and low values of m (low mortality rate) result in higher values of D_{coex} .

From now on, the coexistence equilibrium, whenever it exists, will be denoted by

$$E_c = (x_c, y_c).\tag{14}$$

The following result states some dynamical properties of E_c .

Lemma 2. (*Stability of the coexistence equilibrium*) *Let us define the function $h : (0, \infty) \rightarrow \mathbb{R}$ by*

$$h(x) := \frac{(\mu(x) - D)x}{\nu(x)}.\tag{15}$$

If the coexistence equilibrium E_c exists, then:

- 135 (a) *if $h'(x_c) < 0$, then E_c is a sink (locally stable),*
(b) *if $h'(x_c) = 0$, then E_c is globally stable on $(0, \infty) \times (0, \infty)$*
(c) *if $h'(x_c) > 0$, then E_c is a source (unstable).*

PROOF. See Appendix B. \square

Remark 1 (Existence of limit cycles). Lemma 2 describes the local stability of the coexistence equilibrium. In particular, it states sufficient conditions
140

for the existence of limit cycles, that is, when E_c is unstable. Proving that the instability of E_c is a necessary condition for the existence of limit cycles has been the concern of many authors [28, 29, 30]. However, most of the results are limited to the case when $\mu(x)$ is described by logistic growth. In this work, we do not aim to prove such results for our model, which could be the subject of a completely different work. However, numerical simulations suggest that the instability of E_c is a necessary and sufficient condition for the existence of a limit cycle (see Figure 4).

Lemma 3. *Let h be the function defined by (15). Assume that the coexistence equilibrium E_c exists. If $h'(x_c) > 0$ and the following inequality holds for all $x \in (0, x^*) - \{x_c\}$:*

$$\frac{d}{dx} \left(\frac{\nu(x)h'(x)}{\nu(x) - m - \alpha D} \right) \leq 0. \quad (16)$$

then (1) admits a unique limit cycle, which is globally stable on $(0, \infty) \times (0, \infty)$.

PROOF. Direct application of Theorem 2.2 in [31].

Remark 2 (Uniqueness of limit cycles). Following Lemma 3, we can show numerically that when E_c is unstable, (1) admits a unique limit cycle that is globally stable [15]. Such result is probably not surprising, the multiplicity of limit cycles has only been observed, for example, in the presence of Allee effect on prey [32] or non-monotonic functional responses by predators [33].

4. Static optimal control problem (SOCP)

4.1. Productivity in the absence of grazers

In the absence of predators ($y = 0$), as discussed in the previous section, for any dilution rate $D \in [0, D_{alg}]$, the microalgae concentration converges toward the steady state $x^*(D)$ (defined by (11)). We then define the steady state biomass productivity as follows $P(D) := LDx^*(D)$. This term represents the quantity of microalgae that is produced per unit of area and time when a solution

Table 2: Different notations for the dilution rate.

Notation	Description
D_{alg}	Minimum dilution rate at which microalgae go extinct.
D_{coex}	Minimum dilution rate at which predators go extinct.
D_C	Solution of (17). Dilution rate at which a pure culture of microalgae reaches its maximal productivity.
D_{SOCP}	Conjectured solution of the SOCP (20). Dilution rate at which the contaminated cultures reaches its maximal productivity.
D_{OCP}	Optimal solution of the OCP (24).
\hat{D}	Suboptimal feedback control proposed in this work (see (25)).

of (10) reaches its steady state. The units of $P(D)$ are g/m²/d. The problem of maximizing P can be written as:

$$\begin{aligned} \max_D \quad & P(D), \\ \text{s.t.} \quad & 0 < D < D_{alg}. \end{aligned} \tag{17}$$

It is well known that P reaches the maximum value when the following compensation condition holds [8]:

$$p(I_{out}(x^*(D))) = r. \tag{18}$$

We will denote by D_C the dilution rate at which the equilibrium x^* verifies the compensation condition (18). Thus, D_C is the solution to (17) (The different notations for the dilution rate are summarized in Table 2).

4.2. Productivity in the presence of grazers

To extend the definition of productivity to a culture contaminated by predators, we must take into account the asymptotic behavior of any solution to (1) with positive initial conditions. According to Proposition 1, there is a dilution rate $D_{coex} > 0$ such that for any $D < D_{coex}$ microalgae and predators survive in the long-term. Moreover, they either settle in the coexistence equilibrium E_c or they approach a periodic solution of (1) (see Figure 4). Following Remark 2, we

assume that, when E_c is unstable, there is a unique limit cycle. We will denote the trajectory and period of the limit cycle by (x_p, y_p) and T , respectively.

We define the areal long-term productivity, denoted by $Q(D)$, as

$$\begin{cases} \frac{L}{T} \int_0^T Dx_p(t)dt, & \text{if } E_c \text{ exists and is unstable,} \\ LDx_c, & \text{if } E_c \text{ exists and is stable,} \\ LDx^*, & \text{if } D_{coex} \leq D < D_{alg}. \end{cases} \quad (19)$$

170 The definition of Q accounts for three different types of asymptotic behavior in which microalgae are present; limit cycle, coexistence equilibrium, and equilibrium without grazers (see Figure 4). Note that when the coexistence equilibrium exists and is unstable, Q corresponds to the daily average biomass productivity during the whole period of the limit cycle. In this way, the units of Q are exactly
 175 the same of P , and the productivity along limit cycles can be compared to that provided by equilibria.

We are interested in finding the constant dilution rate that provides the highest value of Q , that is, we want to solve the following optimization problem:

$$\begin{aligned} \max_D \quad & Q(D), \\ \text{s.t.} \quad & 0 < D < D_{alg}. \end{aligned} \quad (20)$$

We will refer to (20) as the *static optimal control problem* (SOCP).

4.3. Limit cycles are not optimal

The following proposition shows that Q cannot be optimal at a coexistence
 180 equilibrium.

Proposition 2. Let D be such that E_c exists and is stable. Then, $Q(D)$ is not the maximum value of Q .

Proof. Let D be such that $E_c = (x_c, y_c)$ exists and is stable and let us assume that Q reaches the maximum at D . Let x^* be such that $\mu(x^*) = D_{coex}$. From the definition of x_c and from Proposition 1, we have

$$\nu(x_c) = \alpha D + m < \alpha D_{coex} + m.$$

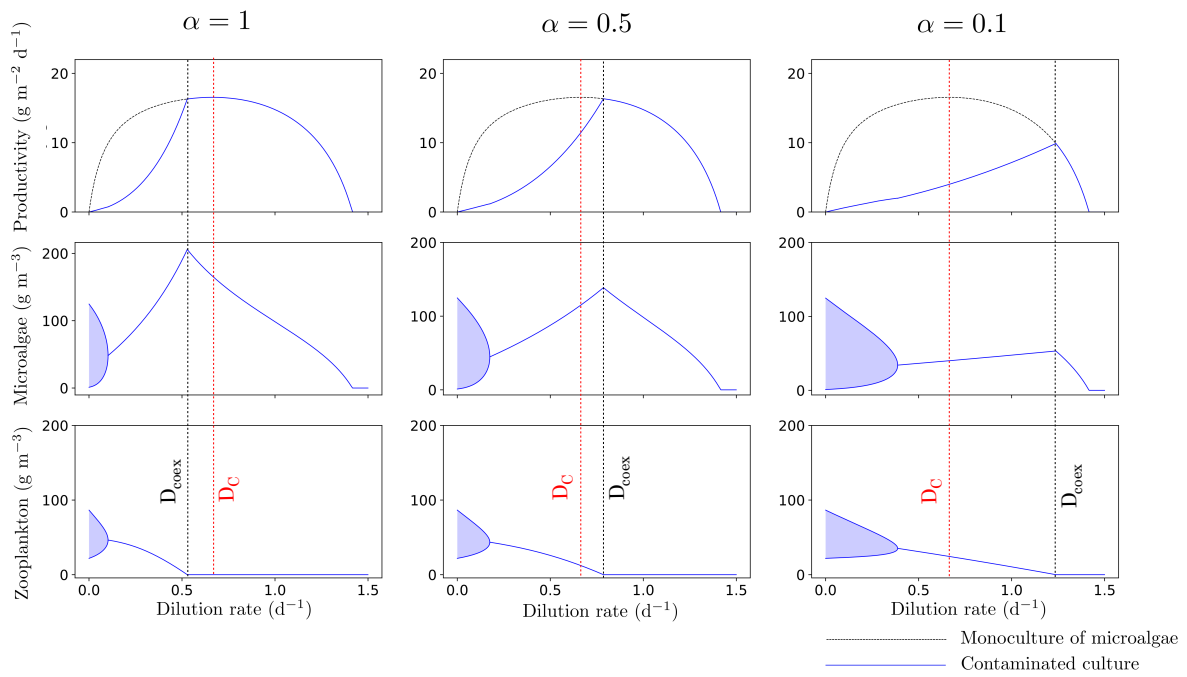


Figure 5: Bifurcation diagram and long-term productivity for different values of α .

From (13), we conclude that

$$\nu(x_c) = \alpha D + m < \nu(x^*).$$

Since ν is strictly increasing, $x_c < x^*$, and consequently $Q(D) < Q(D_{coex})$, which contradicts the hypothesis that Q reaches the maximum at D . \square

185 Proposition 2 states that Q is optimal either at a limit cycle or at an equilibrium without predators (first and third cases in (19)). When dealing with limit cycles, it is not clear how Q behaves. The following Proposition shows that for a constant dilution rate, the microalgal biomass along a limit cycle is higher than that of the unstable coexistence equilibrium.

Proposition 3. Let D be such that (1) admits an unstable coexistence equilibrium $E_c = (x_c, y_c)$. Let (x_p, y_p) be a limit cycle of (1) with period T . We have that

$$x_c < \frac{1}{T} \int_0^T x_p(t) dt. \quad (21)$$

Proof. From the second equation in (1), after dividing both sides by y , we have that

$$\nu(x_c) = m + \alpha D = \frac{1}{T} \int_0^T \nu(x_p(t)) dt.$$

Since ν is strictly concave, applying Jensen inequality [34], we obtain

$$\nu(x_c) < \nu\left(\frac{1}{T} \int_0^T x_p(t) dt\right).$$

190 Finally, since ν is increasing, we obtain (21). \square

In terms of productivity, Proposition 3 states that for an unstable equilibrium $E_c = (x_c, y_c)$, we have that

$$DLx_c < Q(D). \quad (22)$$

Expression (22) is an indicator of the difficulty of arguing that limit cycles cannot be optimal. While we know that coexistence equilibria are not optimal (see Proposition 2), we have no argument to say that the gain in biomass through

a limit cycle cannot surpass the biomass production in the absence of predators.
 195 An answer to the question of whether limit cycles can be optimal or not can be
 numerically investigated.

4.4. Numerical evaluation of the productivity

We use the toolbox Matcont for MATLAB [21] to evaluate numerically the
 productivity Q as a function of the dilution rate. Figure 5 shows a bifurcation
 200 diagram of (1) with respect to the dilution rate and the evaluation of Q . We
 observe a unique value of D at which a Hopf bifurcation takes place, that is,
 when the coexistence equilibrium changes its stability and a limit cycle appears
 [35]. We observe that a reduction of α favors the existence of limit cycles and
 increases the range of dilution rates admitting a coexistence equilibrium. Re-
 205 garding the productivity, we observe that Q is strictly increasing on $[0, D_{coex}]$,
 despite the presence of limit cycles. When grazers are equally diluted as mi-
 croalgae ($\alpha = 1$), D_{coex} is lower than D_C , and D_C is the trivial choice for the
 optimal dilution rate. This dilution rate not only ensures the washout of graz-
 ers, but ensures the highest biomass productivity. When $\alpha = 0.5$ or $\alpha = 0.1$,
 210 D_{coex} is higher than D_C . In this case, D_{coex} is the optimal dilution rate, despite
 the apparent microalgal biomass loss.

Based on our numerical simulations and on the fact that there is no paper
 citing any advantage of predators in microalgal cultivation, we propose the
 following conjecture on the solution of the SOCP.

Conjecture 1. Let D_{coex} be the dilution rate given by Proposition 1 and let
 D_C be the solution to (17). Then, the solution to (20) is given by

$$D_{SOCP} = \max\{D_{coex}, D_C\}. \quad (23)$$

215 To understand Conjecture 1, let us imagine a chemostat with a pure culture
 of microalgae that is operated at optimal dilution rate D_C . We allow then
 the system to reach steady state. Now, let us imagine that a zooplankton
 population invades the culture. If the growth rate of zooplankton is negative,

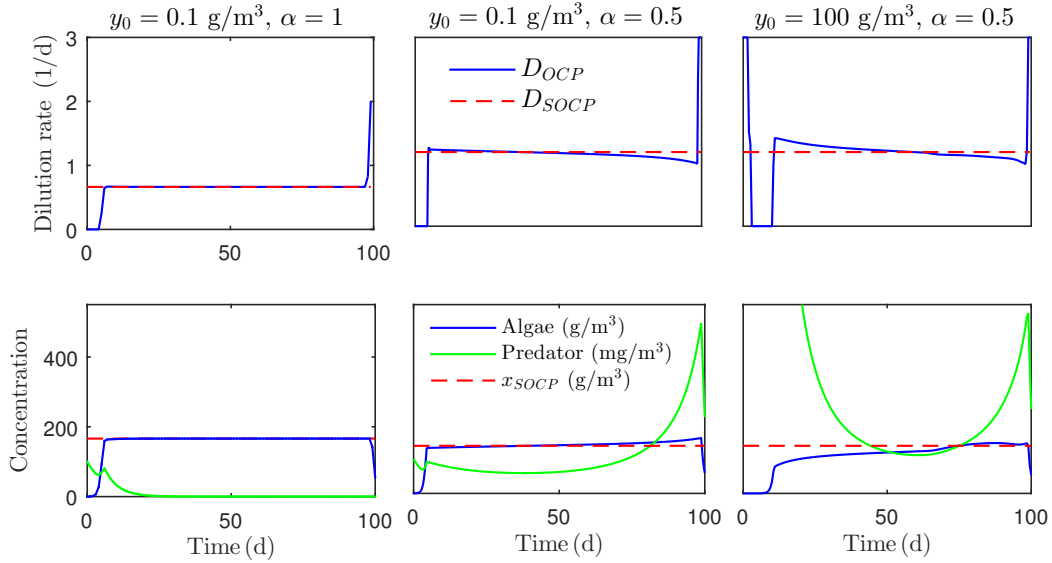


Figure 6: Optimal solution for different initial conditions and values of α . Note that predators and microalgae have different concentration units. Parameters are taken from Table 1 and $x_0 = 0.1 \text{ g/m}^3$.

they will washout and the culture is optimally operated. This corresponds to
220 the case $D_{coex} < D_C$, that is, the optimal dilution rate for the monoculture is
too high to allow the development of zooplankton. On the other hand, if the
invaders have a positive growth rate, they will develop and remain in the culture
in the long-term. In this case, Conjecture 1 states that the dilution rate must
be increased at the minimal value ensuring the washout of predators, that is,
225 the dilution rate must be set at D_{coex} .

5. Optimal control problem (OCP)

5.1. Problem statement

In the previous section, we studied the optimal constant value of the dilution
rate in the long-term operation. In this section, the dilution rate is allowed to
vary in time, and we want to maximize the quantity of biomass that is harvested
on a fixed interval of time $[t_0, t_f]$. We consider the following optimal control

problem (OCP):

$$\begin{aligned}
\max_D \quad & J := \int_{t_0}^{t_f} LD(t)x(t)dt, \\
s.t. \quad & \frac{dx}{dt} = [\mu(x) - D]x - \frac{1}{\gamma}\nu(x)y, \\
& \frac{dy}{dt} = [\nu(x) - m - \alpha D]y, \\
& 0 \leq D(t) \leq D_{max}, \quad t \in [t_0, t_f],
\end{aligned} \tag{24}$$

where D_{max} is the maximal dilution rate allowed. The best policy for $D(t)$ is known as optimal control.

230 Note that the microalgae productivity is given by J and it represents the quantity of biomass (in grams) that is harvested per meter squared in a given interval of time. This productivity is measured in g/m^2 and not $g/m^2/d$ as the productivity Q defined in Section 4. If J is divided by $t_f - t_0$, then we obtain the daily average productivity, which is comparable to Q . However, in
235 this section, we are focus on investigating the structure of the optimal control. For this purpose, it is equivalent to maximizing J or $J/(t_f - t_0)$.

Since D appears linearly in the objective function in (24) and on the system (1), the optimal control is “bang-bang” type, singular, or a combination of both. This follows from the theory of optimal control and the application of
240 the Pontryagin Maximum Principle [36]. When a singular arc takes place, the dilution rate takes intermediate values between 0 and D_{max} . When a bang-bang solution occurs, the optimal control oscillate between 0 and D_{max} .

5.2. Numerical solution

We solve numerically the OCP (24) with a direct method implemented in
245 the software BOCOP [22] (version 2.21). The problem is discretized by a two-stage Gauss-Legendre method of order 4 with 100-500 time steps. We consider a constant initialization, and the tolerance for IPOPTNLP solver is set at 10^{-12} .

Figure 6 shows the optimal solution for different values of α and different initial abundances of grazers. When the initial concentration of grazers is low
250 ($y_0 = 0.1 \text{ g/m}^3$), the structure of the optimal control is bang-singular-bang. That is, at the beginning, the dilution rate is set to zero (bang), then the dilution

rate takes intermediate values between 0 and D_{max} (singular arc), and finally the dilution rate is set to D_{max} (bang). We note that the singular arc is very close to the solution of the SOCP, especially when $\alpha = 1$. When $\alpha = 0.5$ and the initial concentration of predators is high ($y_0 = 100 \text{ g/m}^3$), the optimal control is of the form bang-bang-singular-bang. In this case, an additional switch time is added and the dilution rate is set at its maximum value at the beginning.

5.3. Suboptimal feedback control

Microalgae cultures are generally initiated without zooplankton and with a low concentration of microalgae. In such situations, as suggested by numerical simulations, the solution of the OPC (8) sets the dilution rate to zero at the beginning (see Figure 6). Thus, the microalgae concentration will rapidly increase until reaching a value close to x_{SOCP} . Then, the microalgae concentration stays close to x_{SOCP} while the dilution rate follows a singular arc that is close to D_{SOCP} . Based on this, we propose the following feedback control:

$$\hat{D} = \begin{cases} D_{SOCP} & \text{if } x \geq x_{SOCP}, \\ 0 & \text{if } x < x_{SOCP}, \end{cases} \quad (25)$$

with D_{SOCP} defined by Conjecture 1 and x_{SOCP} defined by the following equation

$$\mu(x_{SOCP}) = D_{SOCP}. \quad (26)$$

The feedback control \hat{D} depends on whether zooplankton can develop or not when the compensation condition (18) holds. If the zooplankton cannot survive, the feedback control leads the process to rapidly satisfy the compensation condition and keeps the system in that state. However, if zooplankton can survive, the strategy consists of forcing microalgae to rapidly reach the lowest equilibrium concentration (x^*) at which they do not support the development of zooplankton ($\nu(x^*) = m + \alpha D$). Then, the system is kept at equilibrium until the end.

This control is not appropriate for initial conditions with a remarkable dominance of grazers in the culture, the application of \hat{D} can result in an oscillatory

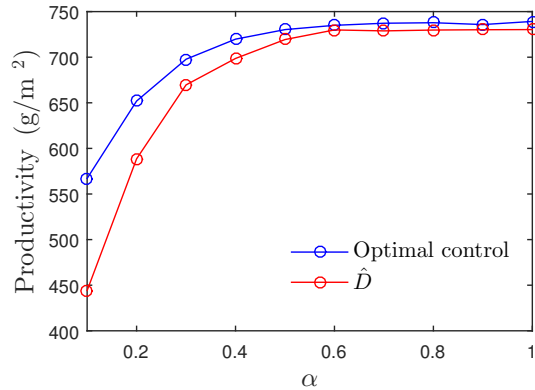


Figure 7: Comparison of the productivity obtained with the optimal control and the feedback control defined by (25). The initial conditions are $x_0 = 0.1 \text{ g/m}^3$ and $y_0 = 0.1 \text{ g/m}^3$ and the interval of time is $[0, 50]$.

behavior in which zooplankton will collapse only after reaching its maximum concentration. As shown in Figure 6, an initial phase with high dilution rate is more suitable for cultures that are already highly contaminated.

Figure 7 shows the productivity associated with \hat{D} and with the optimal control D_{OCP} . We observe that as α increases, both controls give a similar productivity. However, when α is low, the optimal control clearly outperforms the feedback control \hat{D} . When $\alpha = 0.1$, the productivity associated with D_{OCP} is a 27% higher than the productivity associated with \hat{D} . When α is higher than or equal to 0.4, there is an increase of only about 0.5 – 1.5%. This is because low values of α are associated with high values of D_{SOCP} ¹. Thus, when the feedback control sets the dilution rate at D_{SOCP} , there is a loss of microalgae due to dilution that cannot be compensated by the eradication of grazers. For this reason, the optimal control D_{OCP} sets a dilution rate lower than \hat{D} (see Figure 8). This disagreement between both controls is related to time horizon.

¹Indeed, for low values of α , predators are more likely to survive, that is, D_{coex} is higher (see Figure 3). In view of the definition of D_{SOCP} (see (23)), it is clear that D_{SOCP} increases with α .

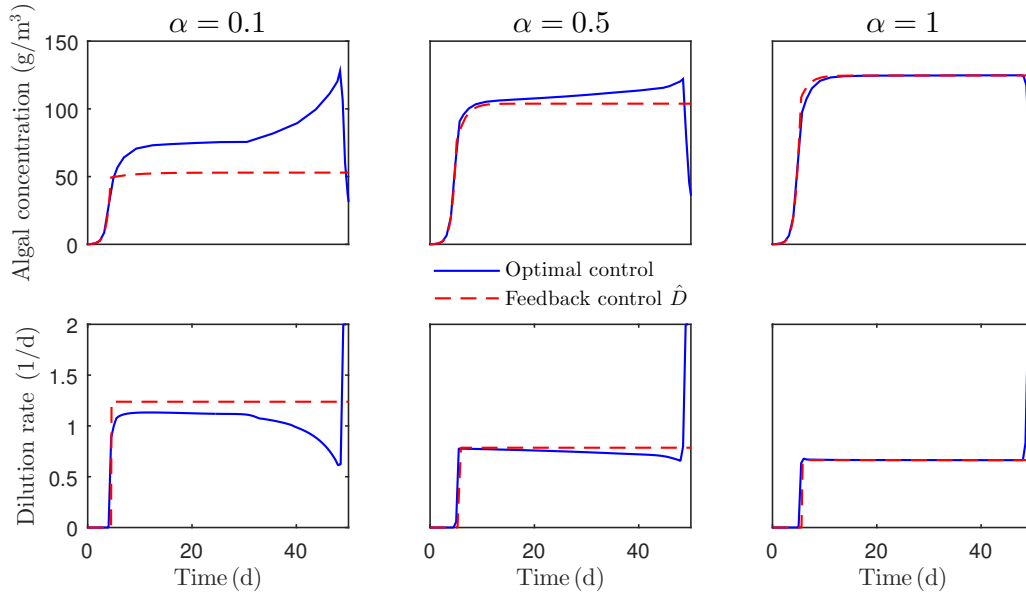


Figure 8: Comparison of the optimal control and \hat{D} on the time interval $[0, 50]$ for different values of α . The initial conditions are $x_0 = 0.1 \text{ g/m}^3$ and $y_0 = 0.1 \text{ g/m}^3$.

290 The construction of \hat{D} is primarily based on the solution of the steady state optimization problem, that is, when the system is operated in large time. As shown in Figure 9, when the time horizon is increased, the optimal control becomes closer to the control \hat{D} . This reveals a Turnpike-like property of the optimal control problem [37]: when the optimal control is settled in large time
 295 intervals, most of the time the optimal control stays close to the solution of the steady state problem. This property becomes more evident when α approaches 1 as shown in Figure 6.

6. Discussion

6.1. Description of the feedback control \hat{D}

300 We have proposed a feedback control of the dilution rate to increase biomass productivity in microalgal cultivation systems that are susceptible to predation. This strategy is sub-optimal but very close to the optimal control when predators

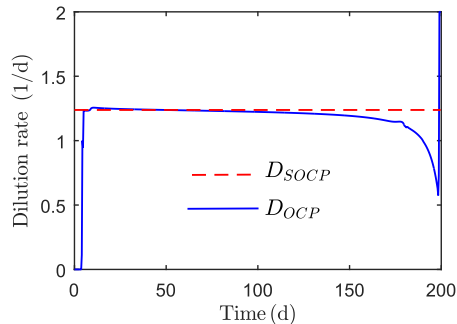


Figure 9: Optimal control when $\alpha = 0.1$ on the time interval $[0, 200]$.

are efficiently diluted (Figure 7, $\alpha \approx 1$) and their initial concentration is low. The efficiency of the feedback control reflects a Turnpike-like property of the optimal control problem [37]: when the optimal control is settled in a large time interval, most of the time the optimal control stays close to the solution of the steady state problem (see Figure 9).

The feedback control \hat{D} is not suitable for highly contaminated systems because setting the dilution rate to zero is not always a good way to rapidly increase microalgae concentration. At fixed low dilution rates, solutions of (1) oscillate approaching a limit cycle (e.g. see Figure 4A). If the initial concentration of grazers is high, the trajectories move counter clock-wise in such a way that the microalgae concentration decreases. Indeed, as shown in Figure 6, the optimal control (D_{OCP}) sets the dilution rate to its maximum value to reduce the abundance of grazers and then sets the dilution rate to zero to increase microalgae density to its optimum steady state value. In future work, the minimum-time control problem of reaching the optimal microalgae density of the SOCP should be addressed. This would allow us to propose a feedback control suitable for any state of the cultivation system.

6.2. Typical start-up of continuous cultures

In real situations, microalgae continuous cultures generally consist of two phases: an initial batch phase (dilution rate equal to zero) in which microalgae

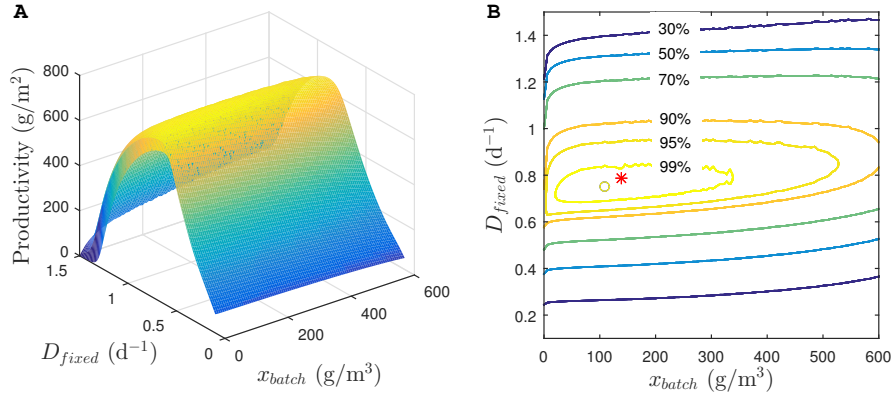


Figure 10: Productivity obtained using the IB control (defined in subsection 6.2) with different values for x_{batch} and D_{fixed} , with $\alpha = 0.5$. **A.** Productivity surface plot. **B.** Level curves of the productivity. The circle (o) represents the optimum choice of x_{batch} and D_{fixed} for the IB control, which provides productivity of 727 g/m². Each level curve represents a percentage of the maximum productivity obtained using the IB control. The star (*) corresponds to the feedback control \hat{D} , that is, $x_{batch} = x_{SOCP}$ and D_{SOCP} .

325 rapidly grow reaching a sufficient cell density, and a second phase in which the reactor is operated at a constant dilution rate [38, 39]. Such control of the dilution rate, henceforth referred to as initial-batch (IB) control (we follow the definition given in [38]), is characterized by two parameters, the microalgae concentration at the end of the batch phase (denoted by x_{batch}) and by a constant dilution rate during the chemostat phase (denoted by D_{fixed}).

330 The feedback control \hat{D} can be seen as an IB control in which x_{batch} is equal to x_{SOCP} (defined by (26)) and D_{fixed} is equal to D_{SOCP} (defined by (23)). A natural question is whether \hat{D} is an efficient control among all the possible IB controls. Figure 10A shows the productivity that is obtained using the IB control with different values of x_{batch} and D_{fixed} . We observe the existence of an optimal combination of x_{batch} and D_{fixed} that maximizes the productivity. The maximal productivity is 727 g/m², and it is reached when $x_{batch} = 109$ g/m³ and $D_{fixed} = 0.75$ d⁻¹. Figure 10B shows the level curves for productivity obtained using the IB control and the productivity associated with $\hat{D}(x)$. We observe that

the feedback control is close to the optimal IB control ($x_{SOCP} = 139 \text{ g/m}^3$ and $D_{SOCP} = 0.79 \text{ d}^{-1}$). The feedback control provides productivity of 724 g/m^2 , that is, a 0.46% lower than the maximum productivity with IB control. This shows that the feedback control \hat{D} is a good approximation of the optimal IB control. Simultaneously, this indicates a good agreement between the optimal IB control and the optimal control D_{OCP} .

6.3. Real implementation of the feedback control

The implementation of the feedback control \hat{D} requires the estimation of three parameters D_{coex} , D_C , and x_{SOCP} . The values of D_C and x_{SOCP} can be estimated from the specific growth rate curve of the microalgae species. The parameter D_C can be also estimated experimentally [10]. Estimating the value of D_{coex} is probably the main difficulty. This parameter depends on the grow capacity of the possible predators, that is, the growth rate of predators, the capacity of predators to escape the outflow, the mortality rate of zooplankton, and factors that were not taken into account in this study, such as temperature. Therefore, dedicated experiments may be needed to estimate D_{coex} , or at least an upper bound.

Once the parameters defining \hat{D} are known, the application of this feedback control is rather conventional: the microalgae culture is operated in batch mode until the system reaches the concentration x_{SOCP} , and then the culture is operated at the dilution rate D_{SOCP} . Different techniques exist for online estimation of the microalgae concentration [40]. This allows the estimation of the moment at which the microalgae concentration is equal to x_{SOCP} . It is important to note that even if this estimation is not precise, the final productivity will not be severely affected. The productivity is rather robust with respect to x_{SOCP} (see Figure 10B).

One advantage of the feedback control \hat{D} is that it does not depend on the population density of grazers. Early detection of zooplankton is not easy, and by the time zooplankton have been detected, it may be too late to optimally operate the system [41].

6.4. Presence of predators in optimal regime

Under constant operation of the chemostat, the optimal dilution rate D_{SOCP} avoids the development of predators. When the dilution rate is allowed to vary in time and the system is run for a finite time, under optimal operation, the presence of grazers depends on their capacity to avoid outflow. If the retention time of zooplankton is notably higher than that for phytoplankton, then some grazers are allowed to stay in the system (see Figure 6 case $\alpha = 0.5$). This is because the benefits of eradicating predators in a short period do not compensate the losses of microalgae due to a high dilution. When grazers are more susceptible to be flushed out from the culture, some grazers may develop but their concentration will remain low for most of the time (see Figure 6 case $\alpha = 1$). Thus, while in the long-term operation predators must be completely avoided, in a finite horizon their eradication may not be optimal.

6.5. Integrated solutions

Microalgae productivity can be increased by implementing the feedback control $hat{D}$ with other techniques to reduce zooplankton contamination. Since x_{SOCP} is determined from (26), the control \hat{D} is completely determined by the value of D_{SOCP} . As shown in Figure 11A, the productivity associated with \hat{D} decreases as the value of D_{SOCP} increases. The reduction of D_{SOCP} is possible by decreasing α or m (see Figure 11B). The reduction of α , can be technologically performed by, for example, placing the outflow closer to where grazers have higher concentrations, or just after the paddle wheel, where individuals are uniformly mixed [6]. Increasing m can be done using methods such as hydrodynamic cavitation [42], increasing CO₂ concentration [43], or even biocontrol using predators for the grazers [4].

7. Conclusion

We have shown the existence of an optimal dilution rate for the steady state operation of continuous microalgae cultures. This optimal dilution rate ensures

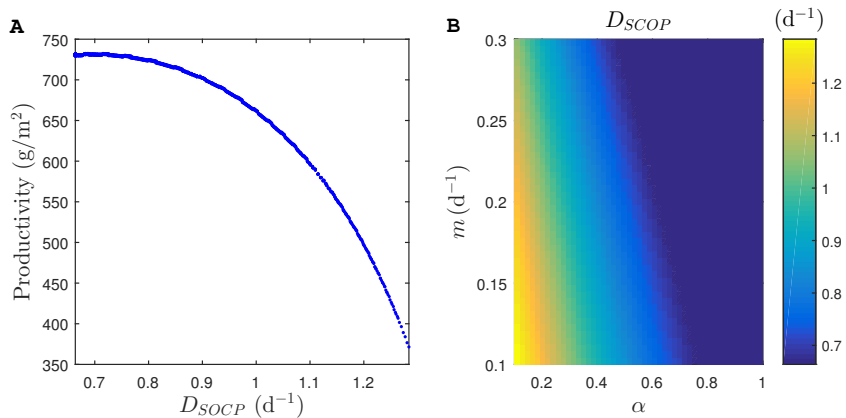


Figure 11: **A.** Productivity using \hat{D} with different values of D_{SOCP} on the interval of time $[0, 50]$ d. **B.** Value of D_{SOCP} for different combinations of α and m .

the eradication of zooplankton, and therefore the productivity cannot be optimal through limit cycles. Another consequence of this is that if predators develop in a microalgae culture, the dilution rate must be increased until avoiding their development. This strategy may not be intuitive because increasing the dilution rate will also negatively affect the microalgae population. However, as shown in the paper, the loss in microalgae through dilution compensates for grazing. It is also important to highlight that such a property is mathematically difficult to prove, and therefore, we used numerical methods to corroborate it.

When the culture is operated during a finite interval of time, we have proposed a simple feedback control for the dilution rate. This feedback control is characterized by an initial batch phase followed by a steady-state operation at optimum dilution rate. This control follows the same structure as typical controls used in real systems, which makes its application possible. Even if this control is not optimal, it is very close to the optimal control when the system is operated for a large period. Finally, this feedback control has the advantage that it depends on the microalgae concentration but not on the grazers concentration. This is important because the early detection of zooplankton is not easy.

Predation during microalgae cultivation has often been neglected while it

415 is one of the most challenging problems at the industrial scale. Its theoretical
 approach has so far rarely been targeted. It is important to account for a longer
 residence time of the predators, which makes the problem even more difficult to
 address. The strategies that we propose are likely to help a practitioner manage
 this issue and avoid the installation of the grazers in the reactor. They must,
 420 however, be associated with a direct treatment, such as biocontrol, to increase
 the predator mortality rate, favoring the proposed control strategy.

Acknowledgements

Carlos Martínez acknowledges the support of the European Union within
 ESIF in the framework of the Operational Programme "Research, Development
 425 and Education" (CZ.02.2.69/0.0/ 0.0/18.053/0016982). Bruno Assis Pessi and
 Olivier Bernard acknowledge the French government through the UCAJEDI
 and EUR DS4H investments in the Future projects managed by the National
 Research Agency (ANR) with the reference numbers ANR-15-IDEX-0001. This
 research work benefited from the support of the FMJH's PGM0 programme
 430 and the support of EDF-THALES-ORANGE to this programme.

Appendix A. Proof of Proposition 1

To prove Proposition 1, we need the following lemma on the boundedness of
 solutions of (1).

Lemma 4 (Boundedness). *Solutions to (1) are bounded.*

PROOF. Let (x, y) be a solution of (1) with $x(0), y(0) > 0$ and let \bar{x} be such
 that

$$\frac{d\bar{x}}{dt} = (\mu(\bar{x}) - D)\bar{x}, \quad \bar{x}(0) = x(0).$$

It is clear that $\bar{x}(t) \leq b := \max\{x(0), x^*\}$ with x^* defined by (11). From a
 comparison argument, it follows that $x(t) \leq \bar{x}(t)$ for all $t \geq 0$, then $x(t)$ is

bounded from above by b . Now, let us define the variable $z = \gamma x + y$. Then we have

$$\frac{dz}{dt} = \gamma\mu(x)x - my - Dz + (1 - \alpha)Dy.$$

Since, $y(t) \leq z(t)$ for all $t \geq 0$, we obtain that

$$\frac{dz}{dt} \leq \gamma\mu(0)b - Dz.$$

435 Then $z(t) \leq b' := \max\{z(0), \gamma\mu(0)b/D\}$ for all $t \geq 0$. It is clear that b' is an upper bound for y which completes the proof. \square

PROOF. (of Proposition 1) For any $D \geq 0$, let us define $x^*(D)$ by means of (11). Now define $\varphi(D) = \nu(x^*(D)) - m - \alpha D$. Note that φ is strictly decreasing, and that $\varphi(0) = \nu(M) - m > 0$ and $\varphi(D_{alg}) = -m - \alpha D_{alg} < 0$. Then, there is a unique $D_{coex} \in (0, D_{alg})$ such that $\varphi(D_{coex}) = 0$. For the part (a), assume that $D < D_{coex}$, then there is $x_c \in (0, x^*(D_{coex}))$ such that $\nu(x_c) = D$. Since μ is strictly decreasing, we have that $\mu(x_c) > \mu(x^*(D_{coex})) = D_{coex} > D$. Consequently,

$$y_c := \gamma \frac{(\mu(x_c) - D)x_c}{\nu(x_c)} > 0.$$

Then the coexistence equilibrium is given by $E_c = (x_c, y_c)$. The uniqueness of E_c follows directly from the monotonicity of ν and μ .

The Jacobian matrix associated with (1) is given by

$$\begin{bmatrix} \mu(x) - D + \mu'(x)x - \frac{1}{\gamma}\nu'(x)y & -\frac{1}{\gamma}\nu(x) \\ \nu'(x)y & \nu(x) - m - \alpha D \end{bmatrix}. \quad (\text{A.1})$$

It is straightforward to verify that $E_0 := (0, 0)$ and E^* are saddle points. Using a stable manifold theorem argument [35], E_0 and E^* can only be reached by solutions starting on $(\{0\} \times \mathbb{R}_+) \cup (\mathbb{R}_+ \times \{0\})$. From Lemma 4, any solution to (1) is bounded. Thus, using the Poincaré-Bendixon Theorem, we conclude that any solution starting on the interior of \mathbb{R}_+^2 approaches asymptotically either E_c or a periodic cycle. For part (b), by contradiction, let $E_c = (x_c, y_c)$ be a coexistence equilibrium. Then

$$\mu(x_c) - \mu(x^*) = \frac{\nu(x_c)}{\gamma x_c} y_c > 0,$$

from where $x_c < x^*$. Now, since $D \geq D_{coex}$ we have

$$0 = \nu(x_c) - m - \alpha D < \nu(x^*) - m - \alpha D = \varphi(D) \leq 0,$$

440 which is a contradiction. Then, there is no coexistence equilibrium. Hence, there is no limit cycle. Consequently, any solution with positive initial conditions approaches either E_0 or E^* . Again, since E_0 is a saddle point, using a stable manifold theorem argument, we conclude that E_0 can only be reached by solutions starting on $\{0\} \times \mathbb{R}_+$. Which completes the proof of (b). Finally, 445 if $D > D_{alg}$, E_0 is the unique equilibrium that (1) admits. Using again the Poincaré-Bendixon Theorem, we conclude that any solution approaches asymptotically E_0 and the part (c) is proved. \square

Appendix B. Proof of Lemma 2

PROOF. The Jacobian matrix associated to (1) evaluated at E_c is given by (see (A.1))

$$J(E_c) = \begin{bmatrix} \mu(x_c) - D + \mu'(x_c)x_c - \frac{1}{\gamma}\nu'(x_c)y & -\frac{1}{\gamma}\nu(x_c) \\ \nu'(x_c)y_c & 0 \end{bmatrix}.$$

Then the trace of $J(E_c)$, denoted τ , and the determinant of $J(E_c)$, denoted δ , are given by

$$\begin{aligned} \tau &= \mu(x_c) - D + \mu'(x_c)x_c - \frac{1}{\gamma}\nu'(x_c)y \quad \text{and} \\ \delta &= \frac{1}{\gamma}x_c y_c f(x_c) \nu'(x_c) > 0. \end{aligned}$$

Thus, if $\tau < 0$, E_c is a sink, if $\tau > 0$, then E_c is a source. If $\tau = 0$, then E_c 450 is a center for the linear system $\frac{d}{dt}(x, y)^T = J(E_c)(x, y)^T$. Then, according to Theorem 5 in Chapter 2.10 in the book of [35], E_c is either a focus, a center, or a center-focus for (1). Choosing appropriately b in Theorem 2.1 in [31], we conclude that there are no limit cycles when $\tau = 0$. Hence, E_c is focus, and consequently stable. From Proposition 1, we conclude the global stability of 455 E_c . Finally, it is straightforward to prove that τ and $h'(x_c)$ have the same sign. This completes the proof. \square

References

- [1] M. Rizwan, G. Mujtaba, S. A. Memon, K. Lee, N. Rashid, Exploring the potential of microalgae for new biotechnology applications and beyond: A review, *Renewable and Sustainable Energy Reviews* 92 (2018) 394–404. doi:<https://doi.org/10.1016/j.rser.2018.04.034>.
460
- [2] D. Molina, J. C. de Carvalho, A. I. M. Júnior, C. Faulds, E. Bertrand, C. R. Soccol, Biological contamination and its chemical control in microalgal mass cultures, *Applied Microbiology and Biotechnology* 103 (23) (2019) 9345–9358. doi:<https://doi.org/10.1007/s00253-019-10193-7>.
465
- [3] E. Molina-Grima, F. García-Camacho, F. G. Ación-Fernández, A. Sánchez-Mirón, M. Plouviez, C. Shene, Y. Chisti, Pathogens and predators impacting commercial production of microalgae and cyanobacteria, *Biotechnology Advances* (2021) 107884doi:<https://doi.org/10.1016/j.biotechadv.2021.107884>.
470
- [4] V. Montemezzani, I. C. Duggan, I. D. Hogg, R. J. Craggs, A review of potential methods for zooplankton control in wastewater treatment High Rate Algal Ponds and algal production raceways, *Algal Research* 11 (2015) 211–226. doi:<https://doi.org/10.1016/j.algal.2015.06.024>.
- [5] M. Schlüter, J. Groeneweg, Mass production of freshwater rotifers on liquid wastes: I. The influence of some environmental factors on population growth of *Brachionus rubens* Ehrenberg 1838, *Aquaculture* 25 (1) (1981) 17–24. doi:[https://doi.org/10.1016/0044-8486\(81\)90095-8](https://doi.org/10.1016/0044-8486(81)90095-8).
475
- [6] V. Montemezzani, I. C. Duggan, I. D. Hogg, R. J. Craggs, Zooplankton community influence on seasonal performance and microalgal dominance in wastewater treatment High Rate Algal Ponds, *Algal Research* 17 (2016) 168–184. doi:<https://doi.org/10.1016/j.algal.2016.04.014>.
480
- [7] N. Hajinajaf, A. Mehrabadi, O. Tavakoli, Practical strategies to improve harvestable biomass energy yield in microalgal culture: A review, *Biomass*

- 485 and Bioenergy 145 (2021) 105941. doi:<https://doi.org/10.1016/j.biombioe.2020.105941>.
- [8] F. Mairet, R. Muñoz-Tamayo, O. Bernard, Adaptive control of light attenuation for optimizing microalgae production, Journal of Process Control 30 (2015) 117–124. doi:<https://doi.org/10.1016/j.jprocont.2015.03.010>.
490
- [9] C. Martínez, O. Bernard, F. Mairet, Maximizing microalgae productivity in a light-limited chemostat, IFAC-PapersOnLine 51 (2) (2018) 735–740. doi:<https://doi.org/10.1016/j.ifacol.2018.04.001>.
- [10] H. Tang, M. Chen, K. Simon Ng, S. O. Salley, Continuous microalgae
495 cultivation in a photobioreactor, Biotechnology and bioengineering 109 (10) (2012) 2468–2474. doi:<https://doi.org/10.1002/bit.24516>.
- [11] H. Qiang, A. Richmond, Productivity and photosynthetic efficiency of *Spirulina platensis* as affected by light intensity, algal density and rate of mixing in a flat plate photobioreactor, Journal of Applied Phycology 8 (2) (1996)
500 139–145. doi:<https://doi.org/10.1007/BF02186317>.
- [12] F. Grognard, A. R. Akhmetzhanov, O. Bernard, Optimal strategies for biomass productivity maximization in a photobioreactor using natural light, Automatica 50 (2) (2014) 359–368. doi:<https://doi.org/10.1016/j.automatica.2013.11.014>.
- 505 [13] R. Muñoz-Tamayo, F. Mairet, O. Bernard, Optimizing microalgal production in raceway systems, Biotechnology Progress 29 (2) (2013) 543–552. doi:<https://doi.org/10.1002/btpr.1699>.
- [14] K. J. Flynn, P. Kenny, A. Mitra, Minimising losses to predation during microalgae cultivation, Journal of applied phycology 29 (4) (2017) 1829–
510 1840. doi:<https://doi.org/10.1007/s10811-017-1112-8>.

- [15] C. Martínez, B. A. Pessi, O. Bernard, Dynamics and productivity of microalgae in presence of predators, *IFAC-PapersOnLine* 54 (3) (2021) 673–678. doi:<https://doi.org/10.1016/j.ifacol.2021.08.319>.
- [16] A. Bhuiyan, S. Akhter, M. Quddus, Diurnal vertical migration of some cladocerans in relation to the physico-chemical factors in a fish pond, *Dhaka University Journal of Biological Sciences* 20 (2) (2011) 147–154. doi:<https://doi.org/10.3329/dujbs.v20i2.8975>.
- [17] U. Sommer, Phosphorus-limited daphnia: intraspecific facilitation instead of competition, *Limnology and Oceanography* 37 (5) (1992) 966–973. doi:<https://doi.org/10.4319/lo.1992.37.5.0966>.
- [18] B. Deruyck, K. H. T. Nguyen, E. Decaestecker, K. Muylaert, Modeling the impact of rotifer contamination on microalgal production in open pond, photobioreactor and thin layer cultivation systems, *Algal Research* 38 (2019) 101398. doi:<https://doi.org/10.1016/j.algal.2018.101398>.
- [19] M. L. Rosenzweig, Paradox of enrichment: destabilization of exploitation ecosystems in ecological time, *Science* 171 (3969) (1971) 385–387. doi:[10.1126/science.171.3969.385](https://doi.org/10.1126/science.171.3969.385).
- [20] G. F. Fussmann, S. P. Ellner, K. W. Shertzer, N. G. Hairston Jr, Crossing the hopf bifurcation in a live predator-prey system, *Science* 290 (5495) (2000) 1358–1360. doi:[10.1126/science.290.5495.1358](https://doi.org/10.1126/science.290.5495.1358).
- [21] A. Dhooge, W. Govaerts, Y. A. Kuznetsov, Matcont: a matlab package for numerical bifurcation analysis of odes, *ACM Transactions on Mathematical Software (TOMS)* 29 (2) (2003) 141–164. doi:<https://doi.org/10.1145/779359.779362>.
- [22] J. Bonnans, V. Grelard, P. Martinon, Bocop, the optimal control solver, open source toolbox for optimal control problems, URL <http://bocop.org> (2011).

- [23] M. Gao, H. Shi, Z. Li, Chaos in a seasonally and periodically forced phytoplankton–zooplankton system, *Nonlinear Analysis: Real World Applications* 10 (3) (2009) 1643–1650. doi:<https://doi.org/10.1016/j.nonrwa.2008.02.005>.
540
- [24] J. Huisman, H. C. Matthijs, P. M. Visser, H. Balke, C. A. Sigon, J. Pargas, F. J. Weissing, L. R. Mur, Principles of the light-limited chemostat: theory and ecological applications, *Antonie van Leeuwenhoek* 81 (1-4) (2002) 117–133. doi:<https://doi.org/10.1023/A:1020537928216>.
545
- [25] C. Martínez, F. Mairet, O. Bernard, Theory of turbid microalgae cultures, *Journal of theoretical biology* 456 (2018) 190–200. doi:<https://doi.org/10.1016/j.jtbi.2018.07.016>.
- [26] O. Bernard, Hurdles and challenges for modelling and control of microalgae for CO₂ mitigation and biofuel production, *Journal of Process Control* 21 (10) (2011) 1378–1389. doi:<https://doi.org/10.1016/j.jprocont.2011.07.012>.
550
- [27] C. Martínez, F. Mairet, O. Bernard, Dynamics of the periodically forced light-limited droop model, *Journal of Differential Equations* (2020). doi:<https://doi.org/10.1016/j.jde.2020.03.020>.
555
- [28] A. Ardito, P. Ricciardi, Lyapunov functions for a generalized gause-type model, *Journal of Mathematical Biology* 33 (8) (1995) 816–828. doi:<https://doi.org/10.1007/BF00187283>.
- [29] M. Hesaaraki, S. Moghadas, Existence of limit cycles for predator–prey systems with a class of functional responses, *Ecological Modelling* 142 (1-2) (2001) 1–9. doi:[https://doi.org/10.1016/S0304-3800\(00\)00442-7](https://doi.org/10.1016/S0304-3800(00)00442-7).
560
- [30] S. Moghadas, B. Corbett, Limit cycles in a generalized gause-type predator–prey model, *Chaos, Solitons & Fractals* 37 (5) (2008) 1343–1355. doi:<https://doi.org/10.1016/j.chaos.2006.10.017>.

- 565 [31] T.-W. Hwang, Uniqueness of the limit cycle for Gause-type predator-prey systems, *Journal of Mathematical Analysis and Applications* 238 (1) (1999) 179–195. doi:<https://doi.org/10.1006/jmaa.1999.6520>.
- [32] E. González-Olivares, H. Meneses-Alcay, B. Gonzalez-Yanez, J. Mena-Lorca, A. Rojas-Palma, R. Ramos-Jiliberto, Multiple stability and uniqueness of the limit cycle in a gause-type predator-prey model considering the Allee effect on prey, *Nonlinear Analysis: Real World Applications* 12 (6) (2011) 2931–2942. doi:<https://doi.org/10.1016/j.nonrwa.2011.04.003>.
- 570 [33] D. Xiao, H. Zhu, Multiple focus and Hopf bifurcations in a predator-prey system with nonmonotonic functional response, *SIAM Journal on Applied Mathematics* 66 (3) (2006) 802–819. doi:<https://doi.org/10.1137/050623449>.
- [34] T. Needham, A visual explanation of Jensen’s inequality, *The American Mathematical Monthly* 100 (8) (1993) 768–771. doi:<https://doi.org/10.1080/00029890.1993.11990484>.
- 580 [35] L. Perko, *Differential equations and dynamical systems*, Vol. 7, Springer Science & Business Media, 2001. doi:<https://doi.org/10.1007/978-1-4613-0003-8>.
- [36] R. B. Vinter, R. Vinter, *Optimal control*, Springer, 2010. doi:<https://doi.org/10.1007/978.0.8176.8086.2>.
- 585 [37] E. Trélat, E. Zuazua, The turnpike property in finite-dimensional nonlinear optimal control, *Journal of Differential Equations* 258 (1) (2015) 81–114. doi:<https://doi.org/10.1016/j.jde.2014.09.005>.
- [38] G. Bougaran, L. Le Déan, E. Lukomska, R. Kaas, R. Baron, Transient initial phase in continuous culture of *isochrysis galbana affinis tahiti*, *Aquatic Living Resources* 16 (4) (2003) 389–394. doi:[https://doi.org/10.1016/S0990-7440\(03\)00053-6](https://doi.org/10.1016/S0990-7440(03)00053-6).
- 590

- [39] B. D. Fernandes, A. Mota, J. A. Teixeira, A. A. Vicente, Continuous cultivation of photosynthetic microorganisms: approaches, applications and future trends, *Biotechnology Advances* 33 (6) (2015) 1228–1245. doi:<https://doi.org/10.1016/j.biotechadv.2015.03.004>.
595
- [40] I. Havlik, P. Lindner, T. Scheper, K. F. Reardon, On-line monitoring of large cultivations of microalgae and cyanobacteria, *Trends in biotechnology* 31 (7) (2013) 406–414.
- [41] J. G. Day, Y. Gong, Q. Hu, Microzooplanktonic grazers—a potentially devastating threat to the commercial success of microalgal mass culture, *Algal Research* 27 (2017) 356–365. doi:<https://doi.org/10.1016/j.algal.2017.08.024>.
600
- [42] D. Kim, E. K. Kim, H. G. Koh, K. Kim, J.-I. Han, Y. K. Chang, Selective removal of rotifers in microalgae cultivation using hydrodynamic cavitation, *Algal research* 28 (2017) 24–29. doi:<https://doi.org/10.1016/j.algal.2017.09.026>.
605
- [43] M. Ma, D. Yuan, Y. He, M. Park, Y. Gong, Q. Hu, Effective control of *Poteroochromonas malhamensis* in pilot-scale culture of *Chlorella sorokiniana* gt-1 by maintaining co₂-mediated low culture pH, *Algal Research* 26 (2017) 436–444. doi:<https://doi.org/10.1016/j.algal.2017.06.023>.
610